Clays and Clay Minerals, Vol. 32, No. 3, 205–212, 1984.

REGULAR SOLUTION SITE-MIXING MODEL FOR CHLORITES

R. K. STOESSELL

Department of Earth Sciences, University of New Orleans
New Orleans, Louisiana 70148

Abstract—Activity expressions are presented for a six end-member, regular solution, site-mixing model for chlorites. The end members are ideal 14-Å chlorites for which experimental stability data are lacking. Estimates were made of the standard state 25°C and 1 bar molar 3rd law entropies, volumes, and the Maier-Kelley heat capacity coefficients. Experimental stability data from the literature for 14-Å chlorites were used with different sets of exchange energies, for cations on adjacent sites, to compute estimates of the standard state chemical potentials of the end members at 25°C and 1 bar. More experimental data are needed for an adequate definition of the exchange energies and the standard state chemical potentials. The model was applied to diagenesis in clastic reservoirs. Aqueous activity ratios of Mg^{2+}:Fe^{2+} were computed as an equilibrium function of the corresponding molar ratios in authigenic chlorites. The aqueous activity ratio was independent of the chlorite Al content at a constant molar ratio of Mg^{2+}:Fe^{2+} in the chlorite. The model predicts a wide range of molar Mg^{2+}:Fe^{2+} ratios in authigenic chlorites in equilibrium with reservoir fluids. Trends in these molar ratios should be independent of the Al content in the chlorites. The model can be applied directly to 7-Å chlorites when experimental data become available to estimate the various thermodynamic parameters of the 7-Å end members.

Key Words—Chlorite, Diagenesis, Free energy of formation, Solid solution, Stability.

INTRODUCTION

Predictions of chlorite formation within mineral assemblages necessitate knowing the stability as a function of composition. The regular solution site-mixing model presented here was derived for use in diagenetic reservoir studies of 14-Å chlorites. The model is also applicable to 7-Å chlorites. Experimental stability data are lacking, however, for 7-Å chlorites, and they are needed to estimate the model parameters. The thermodynamic formulations do not include stability variations due to the different polytypes. This refinement can be added later after more experimental data become available.

A number of solid solution models have been applied to clays. They include the empirical Tardy and Garrels additive scheme (Tardy and Garrels, 1974) and its modifications (e.g., Nriagu, 1975), the ideal mixing of end-member clays (Tardy and Fritz, 1981), ideal site-mixing (Helgeson and Aagaard, 1983; Aagaard and Helgeson, 1983), regular solution site-mixing with random cation mixing (Stoessell, 1979) and with local electrostatic balance (Stoessell, 1981), and the quasi-chemical approximation (Stoessell, 1981). The major disadvantage to using one of the empirical additive schemes is that the solid-solution compositional range is treated in terms of a possible infinite number of phases instead of a few end members. Random, regular solution site-mixing is presented in this study because such mixing has been shown to produce favorable error cancellation in illites by overestimating both the configurational entropy and the excess enthalpy of mixing (Stoessell, 1981).

CHLORITE END MEMBERS AND ASSUMPTIONS

The six 14-Å chlorites used as end members in this study are ideal minerals for which no experimental stability data are available. With one exception, they have compositions that are commonly observed in 7-Å chlorites and other 1:1 clay minerals. The stabilities of the 7-Å analogues are important reference points in estimating the stabilities of the 14-Å end members.

The end members include amesite (ame), $(Mg_4Al_2)(Si_2Al_2)O_{10}(OH)_8$; chamosite (cha), $(Fe^{2+}{}_4Al_2)(Si_2Al_2)O_{10}(OH)_8$; Fe^{3+}-chamosite (F-c), $(Fe^{2+}{}_4Fe^{3+}{}_2)(Si_2Al_2)O_{10}(OH)_8$; talc-3 brucite (t-b), $(Mg_6)(Si_4)O_{10}(OH)_8$; minnesotaite-3 ferrous hydroxide (m-f), $(Fe^{2+}{}_6)(Si_4)O_{10}(OH)_8$; and pyrophyllite-2 gibbsite (p-g), $(Al_4)(Si_4)O_{10}(OH)_8$. These formulae correspond to the structural units used in this study and contain sufficient cations on 4 tetrahedral sites and 6 octahedral sites to balance 28 negative charges. The first pair of parentheses enclose cations in the octahedral (O and O′) sites; and second pair enclose cations in the tetrahedral (T) sites. The talc-3 brucite end member has the composition of serpentine; the minnesotaite-3 ferrous hydroxide end member, the composition of greenalite; and the pyrophyllite-2 gibbsite end member, the composition of kaolinite.

The general stacking sequence for chlorite is TOTO′ along the c axis. Cations in the tetrahedral and octahedral site classes have site coordination numbers of 3 and 6, respectively. These numbers correspond to the number of adjacent cation sites around each cation. The reader is referred to Deer *et al.* (1962) and Bailey

Copyright © 1984, The Clay Minerals Society

https://doi.org/10.1346/CCMN.1984.0320308 Published online by Cambridge University Press

and Brown (1962) for a discussion of the chlorite structures and polytypes. The present model neglects the stability differences between polytypes.

Cation distributions were computed using the same rules for both the end members and the simulated solid solution. Random mixing of cations was assumed without regard to local electrostatic balance in the tetrahedral and octahedral layers. Cations were not allowed to mix between the tetrahedral and the octahedral layers; however, they were allowed to mix between the O and O′ layers, resulting in identical cation distributions in both octahedral layers. The O′ layer contains only $(OH)^-$ anions, while the O layer contains both O^{2-} and $(OH)^-$ anions. The difference in anions implies a difference in cations; however, an assumption of identical cation distributions is necessary because of the lack of detailed information on cation distributions between the O and O′ layers in natural chlorites. Foster (1962) concluded that an equal distribution of cations was consistent with the increase in basal spacing, d(001), with increase in Si content, and with the conversion between 14-Å and 7-Å chlorites. The general equations derived for the model apply to both 14-Å and 7-Å chlorites because of the equal distribution assumption.

Chlorite compositions were simulated by mixing the six end members to cover the range of natural chlorites reported by Hey (1954), Foster (1962), and Weaver and Pollard (1975). Compositional overlap of the end members allows each chlorite composition to be represented by combinations of mole fractions of a maximum of five end members and often by different sets of end member mole fractions. The six end members, however, are necessary to cover the compositional range between Mg-free and Fe^{2+}-free chlorites.

CHLORITE REGULAR SOLUTION MODEL

The algebraic formulation of a regular solution site-mixing model involves computing the molar configurational entropy of mixing, $\Delta\bar{S}_{conf}$, and writing the molar excess enthalpy of mixing, $\Delta\bar{H}_{mix}$, in terms of the exchange energies which are defined below. The procedure followed here is identical to that used for illites by Stoessell (1979, 1981). Only the results with a brief explanation are given below. Table 1 explains all symbols used in the model, and Table 2 summarizes the cation-site occupancies of the 6 chlorite end members.

The molar free energy of mixing, $\Delta\bar{G}_{mix}$, is defined by Eqs. (1) and 2):

$$\Delta\bar{G}_{mix} = RT\sum_i X_i \ln a_i \qquad (1)$$

and

$$a_i = a^0{}_i\lambda_i \qquad (2)$$

where a_i, $a^0{}_i$, and λ_i are the activity, ideal activity (computed from $\Delta\bar{S}_{conf}$), and the activity coefficient (computed from $\Delta\bar{H}_{mix}$), respectively, of the ith end member. X_i is the mole fraction of the ith end member in the chlorite, and R and T are the universal gas constant and the temperature in °K, respectively. The term $a^0{}_i$ corresponds to the probability of picking at random one structural unit of the ith end member out of the

Table 1. Symbols used in the text.

a, a^0	Activity and ideal activity, respectively
a, b, and *c*	Molar heat capacity coefficients for the Maier-Kelley power function
$\bar{E}\bar{X}$	Molar exchange energy in the Xth site class as defined by Eq. (9)
$\Delta\bar{G}$	Molar free energy
$\Delta\bar{H}$	Molar enthalpy
λ	Activity coefficient
O, O′	Octahedral site classes
μ, μ^0	Chemical potential and standard state chemical potential, respectively
P	Pressure in bars
P	Thermodynamic parameter as defined in text
R	Universal gas constant
$\bar{S}^0$, $\Delta\bar{S}$	Standard state molar third law entropy and molar entropy
T	Tetrahedral site class
T	Temperature in °K
$\bar{V}^0$	Standard state molar volume
X	Mole fraction
$\bar{W}\bar{X}$	Contribution to $\Delta\bar{H}_{mix}$ for one mole of adjacent site interactions in the Xth site class, as used in Eq. (9)
Z	Number of adjacent cation sites
Subscripts	
ame	Amesite end member
cha	Chamosite end member
chl	Chlorite
conf	Configurational
E	Empty site
F-c	Fe^{3+}-chamosite end member
i	End member
m-f	Minnesotaite-3 Fe^{2+} hydroxide end member
mix	Mixing
p-g	Pyrophyllite-2 gibbsite end member
t-b	Talc-3 brucite end member
X	Site class
x,y	Cations on adjacent sites

Table 2. Cation-site occupancies per structural unit in the six end-member chlorites.[1]

Chlorite	Octahedral	Tetrahedral
Amesite	$4Mg^{2+}$, $2Al^{3+}$	$2Si^{4+}$, $2Al^{3+}$
Chamosite	$4Fe^{2+}$, $2Al^{3+}$	$2Si^{4+}$, $2Al^{3+}$
Fe^{3+}-chamosite	$4Fe^{2+}$, $2Fe^{3+}$	$2Si^{4+}$, $2Al^{3+}$
Talc-3 brucite	$6Mg^{2+}$	$4Si^{4+}$
Minnesotaite-3 $Fe(OH)_2$	$6Fe^{2+}$	$4Si^{4+}$
Pyrophyllite-2 gibbsite	$4Al^{3+}$, 2E	$4Si^{4+}$

[1] E indicates an empty site.

https://doi.org/10.1346/CCMN.1984.0320308 Published online by Cambridge University Press

solid solution. Its value is unity when X_i is unity; however, due to compositional overlap of the end members, the value can be nonzero when X_i is zero. As mentioned above, this compositional overlap allows a given chlorite composition to be represented by more than one set of end member mole fractions; however, a^0_i and λ_i are constant for a given chlorite composition. The regular solution expressions for a^0_i are given by Eqs. (3) to (8) in terms of the parameters defined below:

$$a^0_{ame} = A1\ A2\ A3\ A4, \quad (3)$$
$$a^0_{cha} = A1\ A5\ A3\ A4, \quad (4)$$
$$a^0_{F\text{-}c} = A5\ A6\ A3\ A4, \quad (5)$$
$$a^0_{t\text{-}b} = A7\ A8, \quad (6)$$
$$a^0_{m\text{-}f} = A9\ A8, \quad (7)$$
$$a^0_{p\text{-}g} = A10\ A11\ A8, \quad (8)$$

where

$$A1 = (X_{ame} + X_{cha} + 2X_{p\text{-}g})^2,$$
$$A2 = (X_{ame} + 1.5X_{t\text{-}b})^4,$$
$$A3 = (X_{ame} + X_{cha} + X_{F\text{-}c})^2,$$
$$A4 = (2 - (X_{ame} + X_{cha} + X_{F\text{-}c}))^2,$$
$$A5 = (X_{cha} + X_{F\text{-}c} + 1.5X_{m\text{-}f})^4,$$
$$A6 = (X_{F\text{-}c})^2,$$
$$A7 = ((2X_{ame} + 3X_{t\text{-}b})/3)^6,$$
$$A8 = (0.5(1 + X_{t\text{-}b} + X_{m\text{-}f} + X_{p\text{-}g})^4,$$
$$A9 = ((2X_{cha} + 2X_{F\text{-}c} + 3X_{m\text{-}f})/3)^6,$$
$$A10 = (0.5X_{ame} + 0.5X_{cha} + X_{p\text{-}g})^4,$$
$$A11 = X^2_{p\text{-}g}.$$

The end member λ_i expressions for the regular solution model are listed below in Eqs. (10) to (15) in terms of molar exchange energies, $\bar{E}\bar{X}_{x,y}$, defined by Eq. (9):

$$\bar{E}\bar{X}_{x,y} = \bar{W}\bar{X}_{x,y} - 0.5(\bar{W}\bar{X}_{x,x} + \bar{W}\bar{X}_{y,y}). \quad (9)$$

$\bar{W}\bar{X}_{x,y}$ is the contribution to $\Delta\bar{H}_{mix}$ for Avogadro's number of adjacent site interactions between x and y cations and/or empty (E) sites in the Xth site class, e.g., O or T site class. No distinction is made between O and O′ because identical distributions of cations have been assumed in both octahedral site classes.

$$\lambda_{ame} = \exp[(1/RT)[(2/3)Z_O[L1(2 - L2)\bar{E}\bar{O}_{Mg,Fe^{2+}} + (2 - L2)(L3 - 1)\bar{E}\bar{O}_{Mg,Al} + X_{F\text{-}c}(2 - L2)\bar{E}\bar{O}_{Mg,Fe^{3+}} + X_{p\text{-}g}(2 - L2)\bar{E}\bar{O}_{Mg,E} + L1(1 - L3)\bar{E}\bar{O}_{Fe^{2+},Al} - X_{F\text{-}c}L1\bar{E}\bar{O}_{Fe^{2+},Fe^{3+}} - X_{p\text{-}g}L1\bar{E}\bar{O}_{Fe^{2+},E} + X_{F\text{-}c}(1 - L3)\bar{E}\bar{O}_{Al,Fe^{3+}} + X_{p\text{-}g}(1 - L3)\bar{E}\bar{O}_{Al,E} - X_{F\text{-}c}X_{p\text{-}g}\bar{E}\bar{O}_{Fe^{3+},E}] + Z_TL4^2\bar{E}\bar{T}_{Al,Si}]]; \quad (10)$$

$$\lambda_{cha} = \exp[(1/RT)[(2/3)Z_O[(2 - L1)L2\bar{E}\bar{O}_{Mg,Fe^{2+}} + L2(1 - L3)\bar{E}\bar{O}_{Mg,Al} - X_{F\text{-}c}L2\bar{E}\bar{O}_{Mg,Fe^{3+}} - X_{p\text{-}g}L2\bar{E}\bar{O}_{Mg,E} + (L3 - 1)(2 - L1)\bar{E}\bar{O}_{Fe^{2+},Al} + X_{F\text{-}c}(2 - L1)\bar{E}\bar{O}_{Fe^{2+},Fe^{3+}} + X_{p\text{-}g}(2 - L1)\bar{E}\bar{O}_{Fe^{2+},E} + X_{F\text{-}c}(1 - L3)\bar{E}\bar{O}_{Al,Fe^{3+}} + X_{p\text{-}g}(1 - L3)\bar{E}\bar{O}_{Al,E} - X_{F\text{-}c}X_{p\text{-}g}\bar{E}\bar{O}_{Fe^{3+},E}] + Z_TL4^2\bar{E}\bar{T}_{Al,Si}]]; \quad (11)$$

$$\lambda_{F\text{-}c} = \exp[(1/RT)[(2/3)Z_O[(2 - L1)L2\bar{E}\bar{O}_{Mg,Fe^{2+}} - L2L3\bar{E}\bar{O}_{Mg,Al} + (1 - X_{F\text{-}c})L2\bar{E}\bar{O}_{Mg,Fe^{3+}} - X_{p\text{-}g}L2\bar{E}\bar{O}_{Mg,E} + (2 - L1)L3\bar{E}\bar{O}_{Fe^{2+},Al} - (1 - X_{F\text{-}c})(2 - L1)\bar{E}\bar{O}_{Fe^{2+},Fe^{3+}} + X_{p\text{-}g}(2 - L1)\bar{E}\bar{O}_{Fe^{2+},E} + (1 - X_{F\text{-}c})L3\bar{E}\bar{O}_{Al,Fe^{3+}} - X_{p\text{-}g}L3\bar{E}\bar{O}_{Al,E} + X_{p\text{-}g}(1 - X_{F\text{-}c})\bar{E}\bar{O}_{Fe^{3+},E}] + Z_TL4^2\bar{E}\bar{T}_{Al,Si}]]; \quad (12)$$

$$\lambda_{t\text{-}b} = \exp[(1/RT)[(2/3)Z_O[L1(3 - L2)\bar{E}\bar{O}_{Mg,Fe^{2+}} + (3 - L2)(L3)\bar{E}\bar{O}_{Mg,Al} + X_{F\text{-}c}(3 - L2)\bar{E}\bar{O}_{Mg,Fe^{3+}} + X_{p\text{-}g}(3 - L2)\bar{E}\bar{O}_{Mg,E} - L1L3\bar{E}\bar{O}_{Fe^{2+},Al} - X_{F\text{-}c}L1\bar{E}\bar{O}_{Fe^{2+},Fe^{3+}} - X_{p\text{-}g}L1\bar{E}\bar{O}_{Fe^{2+},E} - X_{F\text{-}c}L3\bar{E}\bar{O}_{Al,Fe^{3+}} - X_{p\text{-}g}L3\bar{E}\bar{O}_{Al,E} - X_{F\text{-}c}X_{p\text{-}g}\bar{E}\bar{O}_{Fe^{3+},E}] + Z_T(1 - L4)^2\bar{E}\bar{T}_{Al,Si}]]; \quad (13)$$

$$\lambda_{m\text{-}f} = \exp[(1/RT)[(2/3)Z_O[(3 - L1)L2\bar{E}\bar{O}_{Mg,Fe^{2+}} - L2L3\bar{E}\bar{O}_{Mg,Al} - X_{F\text{-}c}L2\bar{E}\bar{O}_{Mg,Fe^{3+}} - X_{p\text{-}g}L2\bar{E}\bar{O}_{Mg,E} + (3 - L1)L3\bar{E}\bar{O}_{Fe^{2+},Al} + X_{F\text{-}c}(3 - L1)\bar{E}\bar{O}_{Fe^{2+},Fe^{3+}} + X_{p\text{-}g}(3 - L1)\bar{E}\bar{O}_{Fe^{2+},E} - X_{F\text{-}c}L3\bar{E}\bar{O}_{Al,Fe^{3+}} - X_{p\text{-}g}L3\bar{E}\bar{O}_{Al,E} - X_{F\text{-}c}X_{p\text{-}g}\bar{E}\bar{O}_{Fe^{3+},E}] + Z_T(1 - L4)^2\bar{E}\bar{T}_{Al,Si}]]; \quad (14)$$

$$\lambda_{p\text{-}g} = \exp[(1/RT)[(2/3)Z_O[-L1L2\bar{E}\bar{O}_{Mg,Fe^{2+}} + L2(2 - L3)\bar{E}\bar{O}_{Mg,Al} - X_{F\text{-}c}L2\bar{E}\bar{O}_{Mg,Fe^{3+}} + (1 - X_{p\text{-}g})L2\bar{E}\bar{O}_{Mg,E} + L1(2 - L3)\bar{E}\bar{O}_{Fe^{2+},Al} - X_{F\text{-}c}L1\bar{E}\bar{O}_{Fe^{2+},Fe^{3+}} + (1 - X_{p\text{-}g})L1\bar{E}\bar{O}_{Fe^{2+},E} + X_{F\text{-}c}(2 - L3)\bar{E}\bar{O}_{Al,Fe^{3+}} + (X_{p\text{-}g} - 1)(2 - L3)\bar{E}\bar{O}_{Al,E} + X_{F\text{-}c}(1 - X_{p\text{-}g})\bar{E}\bar{O}_{Fe^{3+},E}] + Z_T(1 - L4)^2\bar{E}\bar{T}_{Al,Si}]]; \quad (15)$$

https://doi.org/10.1346/CCMN.1984.0320308 Published online by Cambridge University Press

Table 3. Estimated thermodynamic parameters for end-member chlorites.

Chlorites	$\bar{S}^0$ cal/mole/°K	$\bar{V}^0$ cm³/mole	a cal/mole/°K	b × 10³ cal/mole/°K²	c × 10⁻⁵ cal°K/mole
Amesite	109	205	173	35	42
Chamosite	133	204	170	51	38
Fe^{3+}-chamosite	148	219	209	8	38
Talc-3 brucite	110	213	152	63	35
Minn.-3 $Fe(OH)_2$	150	221	163	65	31
Pyr.-2 gibbsite	102	199	146	58	43

where $Z_T = 3$, $Z_O = 6$, and

$$L1 = 2X_{cha} + 2X_{F\text{-}c} + 3X_{m\text{-}f},$$
$$L2 = 2X_{ame} + 3X_{t\text{-}b},$$
$$L3 = X_{ame} + X_{cha} + 2X_{p\text{-}g},$$
$$L4 = X_{t\text{-}b} + X_{m\text{-}f} + X_{p\text{-}g}.$$

ESTIMATED PARAMETERS FOR THE MODEL

The molar free energy of formation of a chlorite, $\Delta\bar{G}_{chl}$, is given by Eq. (16) in terms of the chemical potentials, μ_i, of the end members:

$$\Delta\bar{G}_{chl} = \sum_i X_i\mu_i. \quad (16)$$

As usual, μ_i is defined in terms of the standard state chemical potential, μ^0_i, and a_i:

$$\mu_i = \mu^0_i + RT \ln a_i. \quad (17)$$

In this study, $\bar{E}\bar{X}_{x,y}$, is assumed to be independent of P and T. The PT independence of a^0_i follows from $\Delta\bar{S}_{conf}$ being independent of pressure and temperature. Application of the model involves computing μ^0_i at the PT point of interest and using the set of 11 exchange energies to compute a_i. The following standard-state molar thermodynamic parameters at 25°C and 1 bar are needed for each of the six end members: μ^0_i, $\bar{S}^0_i$ (the molar 3rd law entropy), $\bar{V}^0_i$ (the molar volume, assumed constant), and a, b, and c (the molar heat capacity coefficients for the Maier-Kelley power function). These parameters can then be input into a standard computer program such as "Maddog" (Stoessell, 1977, used in this study) or "Supcrt" (Helgeson *et al.*, 1978) to compute μ^0_i as a function of P and T. These programs use the equations of state for aqueous species developed by Helgeson and his coworkers (Helgeson and Kirkham, 1974a, 1974b, 1976; Helgeson *et al.*, 1981; and Walther and Helgeson, 1977) to compute end-member hydrolysis constants.

$\bar{S}^0_i$, $\bar{V}^0_i$, and Maier-Kelley heat capacity coefficients

Estimates of $\bar{S}^0_i$, $\bar{V}^0_i$, and the Maier-Kelley heat capacity coefficients at 25°C and 1 bar are listed in Table 3. Procedures followed in obtaining the estimates are given below for each of the end members. Unless otherwise stated, all literature data used in the estimations were taken from the internally consistent thermodynamic data base compiled by Helgeson and his coworkers (Helgeson *et al.*, 1978).

Parameters for the amesite end member are those reported for 14-Å amesite. Maier-Kelley heat capacity coefficients for the chamosite end member are those for 7-Å chamosite. $\bar{S}^0_{cha}$ and $\bar{V}^0_{cha}$ were obtained by correcting the 7-Å chamosite values using the percentage difference between 7-Å and 14-Å daphnite values.

The following algorithm was used to estimate parameters (P) for the Fe^{3+}-chamosite end member.

$$P_{F\text{-}c} = P_{14\text{-Å chamosite}} - (4/3)P_{gibbsite} - (1/3)P_{corundum} + (4/3)P_{ferric\ hydroxide} + (1/3)P_{hematitie}.$$

$\bar{S}^0_{ferric\ hydroxide}$ was taken from Wagman *et al.* (1969). $\bar{V}^0_{ferric\ hydroxide}$ and the heat-capacity coefficients were estimated from the following:

$$P_{ferric\ hydroxide} = (1/2)P_{hematite} + (3/2)P_{water},$$

in which the Maier-Kelley heat-capacity coefficient for water was from Kelley (1960).

Heat-capacity coefficients used for the remaining 3 end members are those of the 7-Å analogues of the compositional units (chrysotile, greenalite, and kaolinite). For $\bar{S}^0_i$ and $\bar{V}^0_i$, the 7-Å parameters were corrected using percentage differences between available 7-Å and 14-Å chlorites having the closest compositions. These were clinochlore, daphnite, and amesite, respectively, for the talc-3 brucite, minnesotaite-3 ferrous hydroxide, and pyrophyllite-2 gibbsite end members.

$\bar{E}\bar{X}_{x,y}$

The absolute magnitude of $\bar{E}\bar{X}_{x,y}$ should probably not exceed $2RT/Z_X$, which is a general limit for a regular solution model with zero excess entropy of mixing (Guggenheim, 1952). For diagenetic temperatures (between 25° and 200°C), these magnitudes are approximately 250 and 500 cal/mole, respectively, for the O and T site classes. This results in the absolute contribution to $\Delta\bar{G}_{chl}$ from the 11 exchange energies in $\Delta\bar{H}_{mix}$ being generally less than 1 kcal. In contrast, $\Delta\bar{G}_{chl}$ is of the order of −1800 kcal as shown by experimental data from Kittrick (1982). For this reason, the exchange energies were arbitrarily fixed and the available ex-

https://doi.org/10.1346/CCMN.1984.0320308 Published online by Cambridge University Press

Table 4. Corresponding sets of $\bar{E}\bar{X}_{x,y}$ and estimated μ^0_i values at 25°C and 1 bar.

	Molar exchange energies in cal/mole										
Sets	Al,Si	Al,E	Fe^{3+},E	Mg,Fe^{2+}	Mg,E	Fe^{2+},E	Al,Fe^{3+}	Mg,Al	Mg,Fe^{3+}	Fe^{2+},Al	Fe^{2+},Fe^{3+}
1	0	0	0	0	0	0	0	0	0	0	0
2	−250	−125	−125	0	−125	−125	0	−125	−125	−125	−125
3	−500	−250	−250	0	−250	−250	0	−250	−250	−250	−250
4	−500	−125	−125	0	−125	−125	0	−125	−125	−125	250

	μ^0_i in cal/mole					
Sets	Amesite	Chamosite	Fe^{3+}-cham.	Talc-3 brucite	Minn.-3Fe(OH)$_2$	Pyr.-2 gibb.
1	−1,978,340	−1,713,210	−1,524,220	−1,943,100	−1,545,400	−1,785,900
2	−1,977,660	−1,712,890	−1,524,880	−1,943,160	−1,546,020	−1,783,220
3	−1,976,980	−1,712,580	−1,525,530	−1,943,210	−1,546,610	−1,780,550
4	−1,976,730	−1,712,530	−1,522,880	−1,943,710	−1,547,410	−1,782,600

perimental data used to evaluate μ^0_i. As shown in Table 4, however, the estimated set of μ^0_i values will vary significantly for different sets of $\bar{E}\bar{X}_{x,y}$. More experimental data are needed to refine these values.

Several sets of exchange energies are given in Table 4. The first set of zero values corresponds to ideal site-mixing. The second set is based on a consideration of local charge balance. $\bar{E}\bar{X}_{x,y}$ was made zero when x and y had the same charge. The other exchange energies were arbitrarily fixed at ½ their maximum possible negative values. These adjacent interactions were assumed favored in the O layer because they compensate for the local charge imbalance resulting from either Al substitution for Si in the T layer or the presence of two adjacent empty sites. $\bar{E}\bar{T}_{Al,Si}$ was assumed negative because of the common Al substitution for Si in natural clays. Exchange energies in the third set are fixed at twice those in the second set. With two exceptions, the exchange energies in the fourth set are equivalent to those in the second set. $\bar{E}\bar{T}_{Al,Si}$ and $\bar{E}\bar{O}_{Fe^{2+},Fe^{3+}}$ were fixed at their maximum negative and positive limits, respectively, reflecting the common substitution of tetrahedral Al for Si and the uncommon occurrence of both Fe^{2+} and Fe^{3+} together in significant amounts in natural clays.

μ^0_i for the end members

Sets of the six end-member μ^0_i values at 25°C and 1 bar were estimated using the four chlorite solubilities reported by Kittrick (1982), the estimated clinochlore value of Helgeson *et al.* (1978), the compositional constraint due to overlap of end member compositions, $\Delta\bar{S}_{conf}$, and the different sets of $\bar{E}\bar{X}_{x,y}$. Experimental values of $\Delta\bar{G}_{chl}$ reported by Kittrick were recalculated from the reported solubilities using the data base of Helgeson *et al.* (1978). The updated values of $\mu^0_{Fe^{2+}}$ and $\mu^0_{Fe^{3+}}$ from the 1/31/83 data file for "Supcrt" were used in these recalculations (H. C. Helgeson, University of California, Berkeley, California, personal communication, 1983). Formulae reported by Kittrick were not in precise electrical neutrality, necessitating an arbitrary correction which was made by adding sufficient Si (between 0.0025 and 0.0125 atoms per structural unit) to provide electrical neutrality. The recalculated $\Delta\bar{G}_{chl}$ values, in cal/mole, were −1,872,370 for the Vermont chlorite, −1,882,460 for the Quebec chlorite, and −1,750,240 for the Michigan chlorite, and −1,754,390 for the New Mexico chlorite.

The procedure for estimating μ^0_i involved writing $\Delta\bar{G}_{chl}$ in terms of the regular solution model for each of the five chlorites of known stability and for an additional chlorite of arbitrary composition. An arbitrary assumption of $\Delta\bar{G}_{chl}$ for the unknown stability was made. The six expressions form a set of six linear equations with six unknowns, the μ^0_i values. Matrix algebra was used to solve for the solution set of μ^0_i which was then recalculated using different sets of mole fractions of end members to define the same six chlorites. The value of $\Delta\bar{G}_{chl}$ for the chlorite of unknown stability was varied by an iterative procedure, until a solution set of μ^0_i was found that was nearly independent of which set of mole fractions was used to define the six chlorite compositions. For each set reported in Table 4, μ^0_{ame}, μ^0_{cha}, $\mu^0_{t\text{-}b}$, and $\mu^0_{m\text{-}f}$ are average values in which the total range was within 40 cal. The ranges for $\mu^0_{f\text{-}c}$ and $\mu^0_{p\text{-}g}$ were within 200 and 125 cal, respectively.

The differences between the sets of μ^0_i in Table 4 result from using different sets of $\bar{E}\bar{X}_{x,y}$. The effect of doubling the exchange energies is shown between sets 2 and 3. There was no significant difference in consistency between the four solution sets. Two of the end members, talc-3 brucite and pyrophyllite-2 gibbsite, have 7-Å analogues, kaolinite and chrysotile, for which the standard-state free energies of formation at 25°C and 1 bar are known (Helgeson *et al.*, 1978). Unlike chrysotile, kaolinite readily forms at 25°C; presumably, kinetic constraints inhibit the low-temperature formation of chrysotile, like most pure magnesium silicates (e.g., see Stoessel and Hay, 1978). The $\mu^0_{p\text{-}g}$ values in Table 4 are 25–30 kcal more positive than $\Delta\bar{G}^0_f$ of

https://doi.org/10.1346/CCMN.1984.0320308 Published online by Cambridge University Press

kaolinite. This is consistent with the absence of a 14-Å chlorite of kaolinite composition in nature.

DISCUSSION

The chemical controls on authigenic chlorites in diagenesis are complex and cannot be answered in this report; however, the model can be used to put constraints on the aqueous activity ratios of Mg^{2+}:Fe^{2+} associated with chlorites. For a chlorite to be stable, the end members must be at equilibrium with the solution and hence, with each other. Pure trioctahedral chlorites, lacking Fe^{3+}, are composed of amesite, chamosite, the talc-3 brucite, and the minnesotaite-3 $Fe(OH)_2$ end members. The following reactions can be written between these end members to define the $a_{Mg^{2+}}$:$a_{Fe^{2+}}$ ratios.

$$Fe^{2+}{}_4Al_2(Si_2Al_2)O_{10}(OH)_8 + Mg_6Si_4O_{10}(OH)_8 + 2Fe^{2+} = Mg_4Al_2(Si_2Al_2)O_{10}(OH)_8 + Fe^{2+}{}_6Si_4O_{10}(OH)_8 + 2Mg^{2+} \quad (a)$$

$$Mg_4Al_2(Si_2Al_2)O_{10}(OH)_8 + 4Fe^{2+} = Fe^{2+}{}_4Al_2(Si_2Al_2)O_{10}(OH)_8 + 4Mg^{2+} \quad (b)$$

$$Mg_6Si_4O_{10}(OH)_8 + 6Fe^{2+} = Fe^{2+}{}_6Si_4O_{10}(OH)_8 + 6Mg^{2+} \quad (c)$$

The Fe^{3+}-chamosite end member has been omitted from the reactions, because another mineral would be needed to set the activity of Fe^{3+}.

The aqueous activity ratio of Mg^{2+}:Fe^{2+} in equilibrium with a given chlorite composition at a particular PT point can be computed from reactions (a), (b), and (c) using each of the four data sets in Table 1. Exchange energies used in the computations are $\bar{E}\bar{T}_{Al,Si}$, $\bar{E}\bar{O}_{Mg,Fe^{2+}}$, $\bar{E}\bar{O}_{Mg,Al}$, $\bar{E}\bar{O}_{Fe^{2+},Al}$. Activity coefficients, computed from the exchange values of each set in Table 4, cancel out in the activity quotients in the reaction for a given chlorite composition. This cancellation is due to stoichiometry of the reactions, setting $\bar{E}\bar{O}_{Mg,Fe^{2+}}$ to zero, and assuming equal values of $\bar{E}\bar{O}_{Mg,Al}$ and $\bar{E}\bar{O}_{Fe^{2+},Al}$. Thus, differences in computed aqueous activity ratios of Mg^{2+}:Fe^{2+}, between the different data sets, depend only on the sets of μ^0_i values. The maximum differences in computed ratios for a given composition were less than 0.16 log units for the PT conditions shown on Figure 1, reflecting the success in satisfying the experimental constraints in deriving each set of μ^0_i values in Table 1. The curves marked "a," "b," and "c" on Figure 1 were derived using the first data set in Table 1.

Curves "b" and "c" should overlap with curve "a" at each PT point. The curves did overlap at 25°C and 1 bar; however, they began to separate with increasing P and T. The separation is due to errors in computing μ^0_i from the estimated standard state parameters in Table 2. These errors produce a total separation of less than 0.2 log units at 150°C and 500 bars.

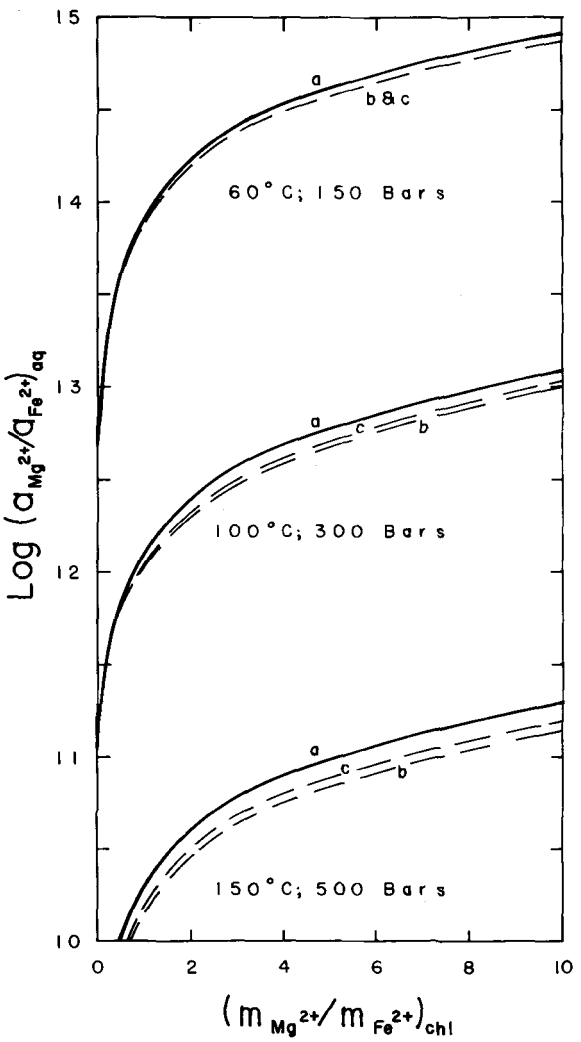


Figure 1. Log $a_{Mg^{2+}}/a_{Fe^{2+}}$ in solution vs. molar Mg:Fe^{2+} ratios in chlorites as computed from end member equilibria. Curves "a," "b," and "c" refer to reactions (a), (b), and (c) in the text.

Changing the Al content in the 4 end member solid solution, while holding the molar Mg:Fe^{2+} ratio constant, did not affect the $a_{Mg^{2+}}/a_{Fe^{2+}}$ ratio. This was due to compensating changes in both the end member ideal activities and in the activity coefficients in the activity quotient for each of the three reactions. Because of the independence of Al content, curves "b" and "c" apply directly to the binary solid solutions of amesite and chamosite and of talc-3 brucite and minnesotaite-3 ferrous hydroxide, respectively.

The three PT points on Figure 1 are 60°C and 150 bars, 100°C and 300 bars, and 150°C and 500 bars. These points fall on a hydrostatic gradient of about

https://doi.org/10.1346/CCMN.1984.0320308 Published online by Cambridge University Press

0.8°C/30 m. The change in log $a_{Mg^{2+}}/a_{Fe^{2+}}$ over a change of 1 to 9 in the molar ratio of Mg^{2+}:Fe^{2+} in the chlorite, is about one log unit at each PT point. At these temperatures, the $a_{Fe^{2+}}$ is probably controlled by reactions with iron oxides, iron sulfides, and iron-rich carbonates. The controlling aqueous activities would be the pe, a_{HS^-}, $a_{CO_3^{2-}}$, and the pH. Small "noncompensating" changes in these factors would have a large effect on the $a_{Mg^{2+}}$:$a_{Fe^{2+}}$ ratio and subsequently produce a large change in the Mg^{2+}:Fe^{2+} molar ratio in a precipitating chlorite. Assuming a lack of re-equilibration due to reaction kinetics, these molar ratios may be preserved in reservoir chlorites. Hence, a wide range in chlorite compositions in reservoirs may be expected. Trends in molar ratios of Mg^{2+}:Fe^{2+} are not expected to be related to trends in Al content, assuming similar values for $\bar{E}\bar{O}_{Mg,Al}$ and $\bar{E}\bar{O}_{Fe^{2+},Al}$. This conclusion is supported by Alford's (1983) study of authigenic chlorite compositions in the Gulf Coast Tuscaloosa Formation.

The estimated thermodynamic parameters in Tables 3 and 4 are consistent enough to compute $\Delta\bar{G}_{chl}$ for plotting approximate stoichiometric chlorite stability fields on phase diagrams. This use is conditional, of course, on the reliability of the experimental data base used to compute those parameters (Kittrick, 1982; Helgeson *et al.*, 1978; and the 1/31/83 "Supcrt" update from Helgeson, personal communication, 1983). The effect of using different data sets in Table 4 to compute $\Delta\bar{G}_{chl}$ for a given chlorite composition will be small, because $\Delta\bar{G}_{mix}$ is small compared to the total free energy of formation of the chlorite.

For writing reactions between certain end members, the computed equilibrium conditions are nearly independent of which data set is used in Table 4. This independence occurs for reactions (a), (b), and (c) for the reasons discussed above. The use of different data sets, however, will not necessarily give similar results when used to compute equilibrium constants for reactions between end members and nonchlorite minerals. Unfortunately, these are the reactions which are most useful in defining the stability of chlorites on phase diagrams. Plotting the stability field of chlorite in terms of end-member mole fractions is more reasonable than plotting a large number of stoichiometric chlorite stability fields. More experimental data on chlorite solubility are needed to define the valid set of exchange energies in chlorites.

ACKNOWLEDGMENTS

The author is indebted to the many industry petrologists, such as Alan F. Thomson of Shell Oil Company and Guy W. Smith of Chevron USA, Inc., who have devoted their research efforts to describing chlorite diagenesis in clastic reservoirs. Their efforts have provided geochemists with the observations necessary to begin to delineate chlorite stabilities. The author especially wishes to acknowledge the help of Carol Bruton of Atlantic Richfield Company who corrected the calculations used in deriving Figure 1. In addition, Per Aagaard and an unidentified reviewer, made constructive comments which helped in revising the manuscript.

REFERENCES

Aagaard, P. and Helgeson, H. C. (1983) Activity/composition relations among silicates and aqueous solutions: II. Chemical and thermodynamic consequences of ideal mixing of atoms on homological sites in montmorillonites, illites, and mixed-layer clays: *Clays & Clay Minerals* **31,** 207–217.

Alford, E. V. (1983) Compositional variations of authigenic chlorites in the Tuscaloosa Formation, Upper Cretaceous, of the Gulf Coast Basin: M.S. thesis, Univ. New Orleans, New Orleans, Louisiana, 66 pp.

Bailey, S. W. and Brown, B. E. (1962) Chlorite polytypism: 1. Regular and semi-random one-layer structures: *Amer. Mineral.* **47,** 819–850.

Deer, W. A., Howie, R. A., and Zussman, J. (1962) *Rock Forming Minerals. Vol. 3 Sheet Silicates:* Longman, Hong Kong, 270 pp.

Foster, M. D. (1962) Interpretation of the composition and a classification of the chlorites: *U.S. Geol. Surv. Prof. Pap. 414-A,* A1–A27.

Guggenheim, E. A. (1952) *Mixtures:* Clarendon Press, Oxford, 270 pp.

Helgeson, H. C. and Aagaard, P. (1984) Activity/composition relations among silicates: I. Thermodynamics of intrasite mixing and substitutional order/disorder in minerals: *Amer. J. Sci.* **283** (in press).

Helgeson, H. C., Delany, J. M., Nesbitt, H. W., and Bird, D. K. (1978) Summary and critique of the thermodynamic properties of rock-forming minerals: *Amer. J. Sci.* **278-A,** 1–213.

Helgeson, H. C. and Kirkham D. H. (1974a) Theoretical prediction of the thermodynamic behavior of aqueous electrolytes at high pressures and temperatures. I. Summary of the thermodynamic/electrostatic properties of the solvent: *Amer. J. Sci.* **274,** 1089–1198.

Helgeson, H. C. and Kirkham D. H. (1974b) Theoretical prediction of the thermodynamic behavior of aqueous electrolytes at high pressures and temperatures. II. Debye-Huckel parameters for activity coefficients and relative partial molal properties: *Amer. J. Sci.* **274,** 1199–1261.

Helgeson, H. C. and Kirkham D. H. (1976) Theoretical prediction of the thermodynamic behavior of aqueous electrolytes at high pressures and temperatures. III. Equation of state for aqueous species at infinite dilution: *Amer. J. Sci.* **276,** 97–240.

Helgeson, H. C., Kirkham D. H., and Flowers, G. C. (1981) Theoretical prediction of the thermodynamic behavior of aqueous electrolytes at high pressures and temperatures. IV. Calculation of activity coefficients, osmotic coefficients, and apparent molal and standard and relative partial molal properties to 5 kb and 600°C: *Amer. J. Sci.* **281,** 1249–1516.

Hey, M. H. (1954) A new review of the chlorites. *Mineral Mag.* **30,** 277–292.

Kelley, K. K. (1960) Contributions to the data on theoretical metallurgy. XIII. High-temperature heat content, heat capacity, and entropy data for the elements and inorganic compounds: *U.S. Bur. Mines Bull.* **584,** 232 pp.

Kittrick, J. A. (1982) Solubility of two high-Mg and two high-Fe chlorites using multiple equilibria: *Clays & Clay Minerals* **30,** 167–179.

https://doi.org/10.1346/CCMN.1984.0320308 Published online by Cambridge University Press

Nriagu, J. O. (1975) Thermochemical approximations for clay minerals: *Amer. Mineral.* **60,** 834–839.
Stoessell, R. K. (1977) Geochemical studies of two magnesium silicates, sepiolite and kerolite: Ph.D. thesis, Univ. California at Berkeley, 135 pp.
Stoessell, R. K. (1979) A regular solution site-mixing model for illites: *Geochim. Cosmochim. Acta* **43,** 1151–1159.
Stoessell, R. K. (1981) Refinements in a site-mixing model for illites: local electrostatic balance and the quasi-chemical approximation: *Geochim. Cosmochim. Acta* **45,** 1733–1741.
Stoessell, R. K. and Hay, R. (1978) The geochemical origin of sepiolite and kerolite at Amboseli, Kenya: *Contrib. Mineral. Petrol.* **68,** 255–267.
Tardy, Y. and Garrels, R. M. (1974) A method of estimating the Gibbs energies of formation of layer silicates: *Geochim. Cosmochim. Acta* **38,** 1101–1116.
Tardy, Y. and Fritz, B. (1981) An ideal solid solution model for calculating solubility of clay minerals: *Clay Miner.* **16,** 361–373.
Wagman, D. D., Evans, W. H., Parker, V. B., Halow, I., Bailey, S. S. M., and Schumm, R. H. (1969) Selected values of chemical thermodynamic properties. Tables for elements 35 through 53 in the standard order of arrangement: *Nat. Bur. Stand. Tech. Note* **270-4,** 141 pp.
Walther, J. V. and Helgeson, H. C. (1977) Calculation of the thermodynamic properties of aqueous silica and the solubility of quartz and its polymorphs at high pressures and temperatures: *Amer. J. Sci.* **277,** 1315–1351.
Weaver, C. E. and Pollard, L. D. (1975) *The Chemistry of Clay Minerals:* Elsevier, New York, 213 pp.

(Received 20 January 1983; accepted 30 October 1983)

Резюме—Представлены выражения для активности для модели хлоритов, основанной на шести конечных членах и регулярном растворе. Конечные члены являются идеальными 14 Å хлоритами, для которых экспериментальные данные по стабильности не имеются. Оценивались молярные энтропие (3 закон), объемы и коэффициенты теплоемкости Майера-Келлея для стандартного состояния 25°C и 1 бара. Экспериментальные данные по стабильности, имеюшиеся в литературе для 14 Å хлоритов, использовались с различными энергиями обмена соседних катионов для расчета химических потенциалов конечных членов при стандартном состоянии 25°C и 1 бара. Однако для соответствующего определения энергий обмена и химических потенциалов при стандартном состоянии необходимы дополнительные экспериментальные данные. Эта модель применялась для диагенеза в кластических резервуарах. Рассчитывались отношения водных активностей Mg^{2+}:Fe^{2+} как функции равновесия соответствующих молярных отношений в аутигенных хлоритах. При постоянном молярном отношении Mg^{2+}:Fe^{2+} в хлорите отношение водных активностей не зависило от содержания Al в этом минерале. Эта модель предсказывает широкий диапазон значений молярных отношений Mg^{2+}:Fe^{2+} в аутигенных хлоритах в равновесии с жидкостями резервуара. Тенденции изменений этих молярных отношений не должны зависеть от содержания Al в хлорите. Модель может непосрдственно применяться к 7 Å хлоритам, если имеются экспериментальные данные для определения различных термодинамических параметров 7 Å конечных членов. [E.G.]

Resümee—Aktivitätsausdrücke werden für ein sechs Endglieder enthaltendes, reguläres Lösungs-Platzmischungsmodell für Chlorite angegeben. Die Endglieder sind ideale 14-Å Chlorite, für die es keine experimentellen Stabilitätsdaten gibt. Es wurden Schätzungen für den Standardzustand der molaren (3. Hauptsatz-)Entropie bei 25°C und 1 Bar, das Volumen, und die Maier-Kelley Wärmekapazitätskoeffizienten gemacht. Experimentelle Stabilitätsdaten aus der Literatur für 14-Å Chlorite wurden zusammen mit verschiedenen Austauschenergien für Kationen auf benachbarten Plätzen verwendet, um Schätzungen für die Standardzustände der chemischen Potentiale der Endglieder bei 25°C und 1 Bar zu berechnen. Es werden mehr experimentelle Daten für eine angemessene Definition der Austauschenergien und der Standardzustände der chemischen Potentiale benötigt. Das Modell wurde auf die Diagenese in klastischen Bereichen angewandt. Das Aktivitätsverhältnis in wässriger Lösung war bei einem konstanten molaren Mg^{2+}:Fe^{2+}-Verhältnis im Chlorit unabhängig vom Al-Gehalt des Chlorites. Das Modell sagt einen großen Bereich von molaren Mg^{2+}:Fe^{2+}-Verhältnissen in authigenen Chloriten voraus, die im Gleichgewicht mit den Vorratslösungen sind. Trends in diesen molaren Verhältnissen sollten unabhängig vom Al-Gehalt der Chlorite sein. Das Modell kann direkt auf 7-Å Chlorite angewendet werden, wenn experimentelle Daten zur Vergügung stehen, um die verschiedenen thermodynamischen Parameter der 7-Å Endglieder abzuschätzen. [U. W.]

Résumé—On présente des expressions d'activité pour un modèle à 6 membres terminaux, à solution regulière, et à sites mélangés pour des chlorites. Les membres terminaux sont des chlorites idéales de 14 Å pour lesquelles des données expérimentales de stabilité manquent. On a estimé les entropies de 3eme loi, les volumes, et les coefficients de capacité de rétention de chaleur de Maier-Kelley pour l'état standard à 25°C et 1 bar molaire. Les données expérimentales de stabilité trouvées dans la littérature pour des chlorites de 14 Å ont été utilisées avec différents ensembles d'énergies d'échange, pour des cations sur des sites adjacents, pour computer des estimations de potentiels chimiques à l'état standard des membres terminaux à 25°C et 1 bar. Le modèle a été appliqué à la diagénèse dans des reservoirs clastiques. On a computé les proportions d'activité aqueuse pour Mg^{2+}:Fe^{2+} en tant que fonction d'équilibre des proportions molaires correspondantes dans des chlorites authigéniques. La proportion d'activité aqueuse était indépendante du contenu en chlorite Al pour une proportion molaire constante de Mg^{2+}:Fe^{2+} dans la chlorite. Le modèle prédit une large gamme de proportions molaires Mg^{2+}:Fe^{2+} dans des chlorites authigéniques en équilibre avec les fluides du réservoir. Les tendances dans ces proportions molaires devraient être indépendantes du contenu en Al des chlorites. Le modèle pourra être directement appliqué à des chlorites de 7 Å lorsque l'on aura des données expérimentales pour estimer les paramètres thermodynamiques variés de membres terminaux de 7 Å [D.J.]

https://doi.org/10.1346/CCMN.1984.0320308 Published online by Cambridge University Press